Annals of Biomedical Engineering, Vol. 31, pp. 515–525, 2003
Printed in the USA. All rights reserved.

0090-6964/2003/31(5)/515/11/$20.00

Three-Dimensional Reconstruction of Thrombus Formation during Photochemically Induced Arterial and Venous Thrombosis

TING ZHU,[1,2] HUCHENG ZHAO,[2] JIA WU,[2] and MARC F. HOYLAERTS[1]

[1]Center for Molecular and Vascular Biology, University of Leuven, Leuven, Belgium and [2]Biomechanics Laboratory, Department of Engineering Mechanics, Tsinghua University, Beijing, People's Republic of China

(Received 25 November 2002; accepted 5 February 2003)

Abstract—We have selected a model of photochemically induced thrombosis in hamsters and mice in which thrombus formation is visualized via transillumination and quantified via image analysis. Applying a gray-compensation method, the images of developing thrombi were presently transformed and a three-dimensional (3D) reconstruction of thrombus evolution performed off line. To this end, a nondimensional *Gray-compensated parameter* Gc was calculated. The integrated Gc (IGc) correlated linearly ($r = 0.973$) with the amount of light transilluminated and previously quantified as arbitrary light units. Matching Gc for reconstructed occlusive arterial and venous thrombi with the inner diameters of the hamster carotid artery and femoral vein, enabled the further conversion of IGc to real thrombus volumes, up to 0.14 mm^3 in the carotid artery. In addition to enabling a graphical three-dimensional reconstruction of experimental thrombosis, via image subtraction, the kinetics of thrombus growth were visualized. Thus, platelet-mediated thrombus growth was found to occur randomly in small thrombi, but in larger thrombi, it occurred preferentially in its tailing vortex in areas of recirculating flow. The present study therefore confirms *in vitro* findings in an *in vivo* model. The 3D reconstruction and kinetics of thrombus growth may be helpful in the mechanistic and pharmacological study of experimental thrombosis. © *2003 Biomedical Engineering Society.* [DOI: 10.1114/1.1566771]

Keywords—3D reconstruction, Animal model, Experimental thrombosis, Platelet, Vessel wall, Thrombus volume.

INTRODUCTION

Upon vascular injury, the loss of blood is arrested as a consequence of platelet adhesion to the damaged vessel wall. Adhering platelets further recruit circulating platelets, constituting an aggregate at the damaged site. The simultaneous activation of the coagulation cascade further reinforces this aggregate with a fibrin lattice. Under pathological conditions, the intravascular deregulation of the hemostatic balance can lead to excessive primary and/or secondary hemostasis, causative of thrombotic complications and even vascular occlusion, causing arrest of blood flow and tissue ischemia in vital organs.[5,14] These cardiovascular diseases remain the major health problem in the adult population in many countries.

In the study of various pathogenetic mechanisms involved in arterial and venous thrombosis, and the validation of new potential therapeutical inhibitors of thrombosis, several experimental models of thrombosis have been developed, in large species such as the baboon,[25] pig,[6] and dog,[12] down to small rodents such as the hamster[21,22] and the rat,[4] respectively, the mouse.[1,3] Thrombus formation in such models can be quantified via directly weighing the thrombus formed[1] or via the analysis of variations in the blood flow pattern of thrombosed vessels.[12,25] However, thrombus formation can be visualized directly. Thus, platelet adhesion to the vessel wall has been studied via videomicroscopy in mesenteric arterioles in murine models of thrombosis and atherosclerosis.[8,19]

By applying a technique based on the photochemical induction of thrombosis,[17,23,24] we have adapted an existing model of thrombus formation in the hamster[21,22] and the mouse to study the pharmacological handling of thrombosis and to investigate thrombophilic risk factors in small arteries and veins.[11,18] In this model, a continuous visualization of the developing thrombus is achieved via transillumination of the damaged blood vessel and the size of the growing thrombus is quantified via analysis of the gray value of the transilluminated light.[11,18] Pharmacological[26] and mechanistic[1,10] studies in these models have been performed to address fundamental aspects of thrombosis, as well as for the evaluation of potential antithrombotic drugs.

A three-dimensional (3D) volumetric approach based on laser confocal microscopy, to measure thrombus formation in real time during blood flow in experimental chambers has indicated that synergistic adhesive mechanisms support platelet aggregation and determine the rate of thrombus growth, acting as continuous variables dependent on blood flow conditions.[16] To further extend

Address correspondence to Marc F. Hoylaerts, Center for Molecular and Vascular Biology, Campus Gasthuisberg, Herestraat 49, B-3000 Leuven, Belgium. Electronic mail: Marc.Hoylaerts@med.kuleuven.ac.be

these approaches to include *in vivo* processes reflecting platelet activation and adhesion during pathogenetic mechanisms of arterial and venous thrombosis, we have performed a 3D reconstruction of thrombus formation, induced *in vivo* in our experimental animal models. This approach not only allowed us to reconstruct a dynamic process of thrombus formation in three dimensions, but it also provided us with a tool to calculate true thrombus volumes and to visualize the preferential sites of thrombus growth, as well as its kinetics.

METHODS

Animal Experiments

Animal experiments of thrombosis were performed in the Center for Molecular and Vascular Biology of the KULeuven, Belgium, and were approved by the Institutional Review Board of the University of Leuven. Experiments were performed in accordance with protocols approved by the Institutional Animal Care and Research Advisory Committee and in agreement with the Guidelines for the use of animals in biomedical research.[7] The animals were euthanized at the end of the recording.

The technique used to induce and to monitor mural thrombosis has been described.[11,18] Male and female hamsters (Pfd Gold, University of Leuven, Belgium) weighing 100–150 g were anaesthetized with sodium pentobarbital (60 mg kg^{-1}) i.p. Following induction of anesthesia, animals were placed in a supine position on a heating path at 37 °C. A 2F venous catheter (Portex, Hythe, U.K.) was inserted in the right jugular vein for the administration of Rose Bengal and activators or inhibitors of primary and secondary hemostasis. Then, the right carotid artery (mice and hamsters) or right femoral vein (hamsters) was exposed from the surrounding tissue and mounted on a transilluminator. Immediately after the intravenous administration of Rose Bengal (20 mg kg^{-1}), the exposed segment of femoral vein was irradiated with green light (wavelength 540 nm) using a xenon lamp (L4887, Hamamatsu Photonics, Hamamatsu, Japan), equipped with a heat-absorbing filter and green filter. The light was directed by an optic fiber mounted on a micromanipulator located approximately 5 mm above the intact femoral vein. The transillumination with green light lasted 4 or 5 min in the study, producing a sufficiently large thrombus in control mice or hamsters to be matched with thrombus formation in experimentally treated animals.

Formation and degradation of the thrombus were monitored for 40 min under a microscope at 40 times magnification. The change over time of light transmission through the blood vessel at the site of the trauma was recorded through a microscope-attached camera. Images were recorded in the memory of an attached computer at 10 s intervals during 40 min. Image analysis (Optimas, 6.5) was used to quantify thrombus intensity. From these results, the kinetics of thrombus formation are calculated and the size of the thrombus is expressed in arbitrary units (A.U.) as the total area under the curve, when the light intensity is plotted against time.[11,18] Recorded images were selected and were used as the basis for the present 3D reconstruction. Examples of arterial and venous thrombosis were selected, as performed in the hamster and the mouse, ranging in intensity from weak to occlusive thrombosis.

Optical Analysis: Background

The gray value in the picture conveys the information of the third dimension. Thus, using the gray value at a certain pixel, it is possible to identify the thickness of a thrombus at that specific point. This approach is however complicated by the fact that light transilluminated through a vessel is quickly diffracted, which limits this technique to the detection of thrombosis in small vessels. Thus, we established that the carotid artery of the rabbit is already too thick to enable the study of thrombosis via transillumination (not shown). Nevertheless, the amount of white light transilluminated is proportional to the platelet mass in the thrombus and is quantified by multiplying the average gray value of the treshholded image by the number of selected pixels, to define arbitrary light units (A.U.).

In the present study, in an effort to provide real volumetric information on the thrombus and to eliminate the influence of the vessel wall and blood on the volume estimate, we have made additional adaptations, according to conventional optical theories.[20] To take the diffraction of the vessel into account, as outlined below, we calculated a *compensated* gray value [Gray compensate (Gc)] proportionally related to the real thickness of the thrombus. Because pictures resulting from transillumination provide a projection of the third dimension only, the present 3D reconstruction is done as a bottom-up model.

The *transmissivity* of a thrombus is different from that of blood. Therefore, the gray value conveys information on the thickness of a growing thrombus. To correct this gray value to specifically provide information on the size of the thrombus, the compensated gray value, linearly related to the real thrombus thickness, is defined as

$$\mathrm{Gc} = \ln \frac{P}{P_c}.$$

In this formula, P is the transmitted light intensity at a certain point and P_c represents the transmitted light intensity at a corresponding point on the compensation picture, which is the actual picture taken of the same vessel before thrombus induction. This is schematically illustrated in Fig. 1(a).

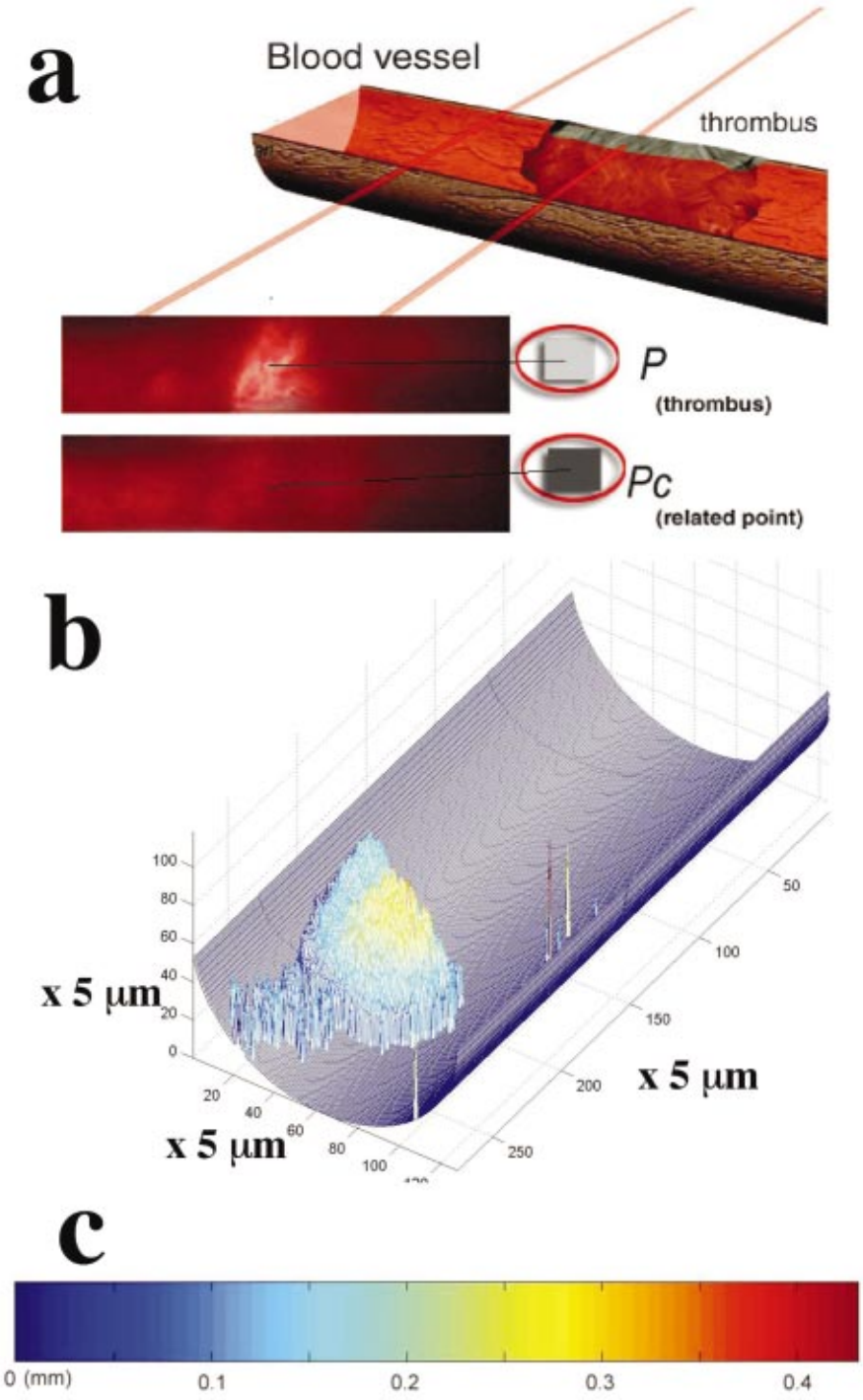

FIGURE 1. Strategy of thrombus 3D reconstruction. Schematic representation of a thrombus in a blood vessel; definition of the thrombus using light transmission intensity *P*, in comparison to the references area with reference light transmission intensity P_c for images obtained via transillumination following photochemical injury of the vessel wall (a); side-view projection of a 3D-reconstructed thrombus in an injured blood vessel (b); graded color scale bar for the representation of the thrombus thickness (c).

According to optical theories, the transmitted light intensity,

$$P = e^{-\mu d},$$

where μ is the transmissivity of the material, and d is its thickness. Now we define P_t, P_v, and P_b, respectively, as the transmitted light intensity for the thrombus (t), the blood vessel (v), and blood (b). According to a similar law μ_t, μ_v, μ_b, d_t, d_v, *and* d_b represent the transmissivity and thickness for thrombus, blood vessel, and blood, respectively. The inner diameter of the vessel is defined as $D = d_t + d_b$; r_v is the reflection loss on the vessel wall, and b represents the intensity of the incident light. The totally transmitted light intensity is then given by

$$P = P_t P_v P_b r_v b = e^{-\mu_t d_t} e^{-\mu_v d_v} e^{-\mu_b d_b} r_v b$$
$$= (e^{-(\mu_v d_v + \mu_b D)} r_v b) e^{-(\mu_t - \mu_b) d_t} = P_c e^{(\mu_b - \mu_t) d_t}. \quad (1)$$

P_c is the transmitted light intensity at a corresponding point on the compensation picture, i.e., position and contrast correlated and, therefore, equals

$$P_c = e^{-(\mu_v d_v + \mu_b D)} r_v b.$$

Following rearranging expression (1), we find the following relation:

$$d_t = \frac{1}{\mu_b - \mu_t} \ln \frac{P}{P_c}, \quad \text{where} \quad \frac{1}{\mu_b - \mu_t} \quad \text{is a constant.}$$

It then follows that $\mathrm{Gc} = \ln(P/P_c)$ is linearly related to the real thickness of the thrombus. Consequently, the integrated number for Gc (**IGc**) is expected to provide information on the real volume of the thrombus.

Optical Analysis: Handling

First, pictures of the developing thrombus were converted into BMP files and then read in Adobe Photoshop (version 6.0), where they were converted into gray pictures, by selecting only the green channel, which provides the best contrast. Pictures from different experiments were then selected for 3D reconstruction, taking care to select the corresponding compensating picture, with light intensity near the base line, i.e., with absent thrombosis.

Selected pictures were then read in Matlab (version 6.1), as a matrix of gray values (P). At the same time, a similar matrix was composed for the compensating picture (P_c). Then, a new matrix is calculated by performing the gray compensation method

$$\mathrm{Gc} = \ln \frac{P}{P_c},$$

i.e., by dividing both matrices and by logarithmically transforming them.

The noise found in Gc in most conditions, mainly due to the localization error (even an anesthetized animal breaths and shows pulsatile blood flow), can be filtered by performing a common widely used median value filtering technique in Matlab (medfilt2). To estimate the reproducibility of this approach, two experimental thrombus pictures were selected and Gc was calculated for a given point in these matrices, using the corresponding background point of six different compensating pictures. After filtering the noise, thus sample 1 yielded a value $\mathrm{Gc} = 38.38 \pm 2.5$ (i.e., SD = 6.51%) and sample 2 yielded $\mathrm{Gc} = 69.88 \pm 3.17$ (i.e., SD = 4.54%).

Also, in Matlab, the filtered Gc matrix was plotted and visualized as a reconstructed image via the mesh function. This is illustrated in Fig. 1(b). To scale the 3D-reconstructed thrombus in the blood vessel, the hamster carotid artery and femoral vein diameter were taken as 450 and 380 μm, respectively, based on microscopic analysis of carotid artery and femoral vein cross sections, containing occlusive thrombosis (not shown) and 3D-reconstructed occlusive thrombi were fitted to these dimensions. Front-views, top- and sideviews were then exported as two-dimensional (2D) images (jpg files). In addition, the sum of all values in the Gc matrix was multiplied by the area per pixel (0.032 mm^2 in the present study, a factor determined by the experimental setup). This yielded a value that corresponds to the integrated Gc, i.e., IGc, which therefore is expressed in mm^2. To further convert IGc into true thrombus volumes, a *conversion factor* was calculated as follows:

$$\frac{\text{Thickness}}{\text{Gc}} = \text{factor} = \frac{\text{Volume}}{\text{IGc}},$$

based on the known fitted thickness for the occlusive thrombi analyzed (blood vessel diameter) and their corresponding Gc, i.e., being expressed in mm. The true volume is then achieved via multiplying this conversion factor and IGc.

In addition to performing the direct volumetric evaluation for the growing thrombus, a kinetic analysis of this process was done to provide an index for the local velocity of thrombus growth. This was done for sequentially taken pictures by subtracting a given matrix describing the local thrombus thickness from the matrix calculated for the preceding image. Thus, an index for the increase of thrombus thickness over a given time interval (defined as growth velocity) was calculated and visualized via its output as a Matlab figure. This analysis was done to study the process of arterial versus venous thrombus growth.

The presently reported analysis was performed on hundreds of pictures derived from 8 independent experiments. Thrombus volume correlation studies between IGc and the original arbitrary light units (A.U.) were done for a single experiment, as outlined below.

RESULTS

Experimental Thrombus Formation

In the arterial circulation, a growing thrombus is confronting constantly increasing mechanical forces, which trigger embolization. As illustrated in Fig. 2(a), in the most ideal manifestation of experimental thrombosis in

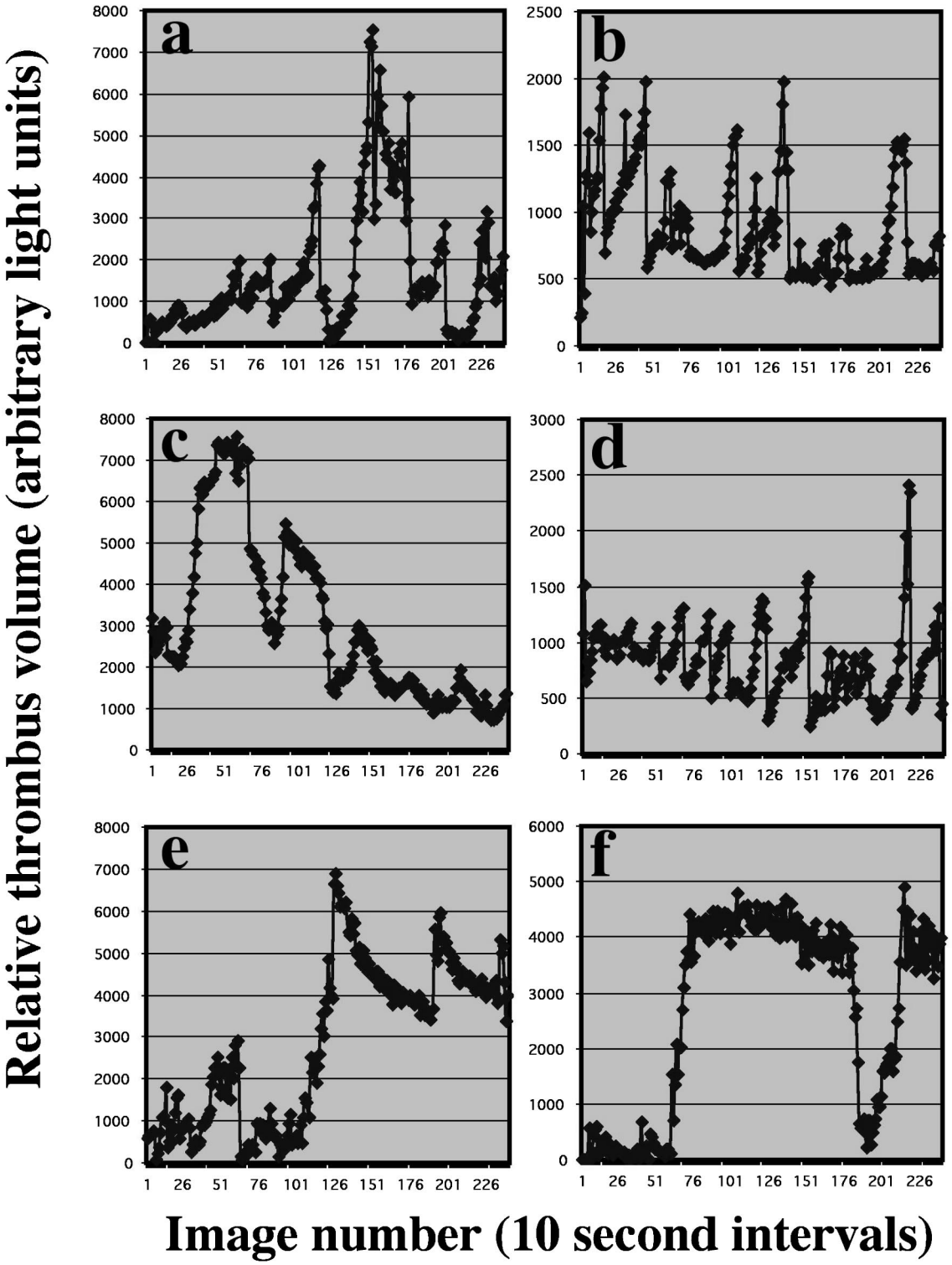

FIGURE 2. Kinetic profiles of thrombus formation in the blood circulation of the hamster. Typical cyclic flow patterns in the carotid artery (a) and (c) and the femoral vein (b) and (d) of the hamster following photochemical injury using Rose Bengal and blood vessel illumination with green light; cyclic flow pattern (e) and stationary thrombosis in the injured carotid artery of the mouse (f).

the hamster carotid artery, this is reflected by a cyclic flow pattern, during which embolization is followed by a rapidly regrowing thrombus. Figure 2(b) shows that also in the hamster femoral vein, thombosis may develop as dictated by a process of cyclic flow variations, although the flow is considerably lower in these conditions. Depending on their size and vessel wall contact, thrombi formed may however be more resistant to flow and show a considerably slower cyclic flow pattern in the hamster carotid artery [Fig. 2(c)]. Figure 2(d) illustrates that even in the presence of 1 $mg\,kg^{-1}$ heparin, cyclic flow variations can be preserved, in agreement with the fact the photochemical induction of vessel wall damage triggers the formation of thrombi rich in platelets, also in the venous circulation. Likewise, the analysis of thrombus formation with time reveals that a cyclic flow pattern can develop in the mouse carotid artery following photochemical injury [Fig. 2(e)], but that also large flow-resistant thrombi can form at comparable levels of experimental injury induction, i.e., upon standardization of the exposure time of the blood vessel to the green light during photochemical injury induction [Fig. 2(f)]. These pictures indicate that experimental thrombosis is controlled by many variables, motivating the present study in which a detailed analysis was made of the type of thrombus formed and of its growth kinetics.

Reconstructing Thrombosis

Figure 3 shows a series of sequential pictures taken during a phase of thrombus growth in the photochemically induced hamster carotid artery. The corresponding 3D-reconstructed pictures are shown in a top-view representation in the second column. The third column shows how the thrombus grows over the experimental time interval of 80 s. Areas displayed in red in the middle column represent zones of highest thrombus thickness, as defined in the color bar in Fig. 1(c). In the right column, the growth velocity is colored as defined in the color bar at the bottom of Fig. 3. The evolution of the calculated IGc over time is shown in Fig. 4(a), in parallel with the evolution of the arbitrary light units [Fig. 4(b)]. Although calculated in an entirely different manner, in agreement with the fact that both IGc and the amount of light units reflect the same process, a strict correlation is found between IGc and A.U. [Fig. 4(c)], described by $y=0.0002202x+0.163(\pm 0.029)$ with a correlation coefficient $r=0.973$. These findings, therefore, validate the mathematical approach followed and justify the further mathematical treatment of the matrices to reconstruct thrombi and calculate derived parameters.

The Gc-based reconstruction for a venous thrombus (Fig. 5) in the femoral vein of the hamster reveals a progressive thrombus development, supported by a progressive growth velocity analysis for the thrombus. The lower panel confirms that upon mathematical conversion, IGc describes this progression with time.

Arterial Versus Venous Thrombus Growth

The detailed analysis of thrombus growth, as illustrated in Fig. 6 shows that thrombus growth preferentially occurred in the tailing vortex of the carotid artery thrombus. This conclusion was drawn after the study of large thrombi in four blood vessels (two hamster carotid artery and two hamster femoral vein thrombi). Growth preference was analyzed by superposing the expanding part of the thrombus (red areas in Fig. 6; velocity >0.01 $mm\,s^{-1}$) onto the thrombus mass itself. Among the reconstructed samples, we further randomly selected 26 (7 arterial versus 19 venous) samples. Most hamster carotid artery thrombi showed a strong growth preference in the tailing vortex, rather than in the areas of the highest thickness, i.e., those areas that are subject to the highest shear rates (engulfed by a black line in Fig. 6; thickness >0.2 mm). Those thrombi developing in the hamster femoral vein showed a fairly random growth: 6/19 grew in the tailing vortex exclusively and 13/19 both in the tailing vortex and thicker thrombus areas (Figs. 5 and 6).

Volume Reconstitution

To enable a correct 3D reconstitution of thrombi formed, Gc needed to be matched to the dimensions of the carotid artery of the hamster. For these purposes, experiments were selected in which occlusive thrombosis was encountered, i.e., sequential pictures indicated a static large thrombus filling the entire lumen at the site of transillumination with no platelet transport. As illustrated in Fig. 7(b), a Gc matrix was calculated for these experiments. This matrix was then scaled to the arterial vessel as illustrated in Fig. 7(c), taking into account the true dimensions of the hamster carotid artery. Following multiple fittings, multiplying the original Gc matrix with a factor 35 provided the best fit, in front view as well as in side-view, using different angles, respectively [Figs. 7(c) and 7(d)].

This fitting further provided the numerical value for the conversion factor. Considering that 80 units in Fig. 7 represent the inner diameter of 0.45 mm, this factor equaled $35\times 0.45\ mm/80=200\ \mu m$ ($\pm 10\ \mu m$). Thus, the product of IGc and this conversion factor, having the dimensions of a volume, enabled calculation of the true thrombus volume. Thus, the occlusive thrombosis shown in Fig. 7(b) was found to yield a thrombus volume up to 0.14 mm^3 [Fig. 8(a)] and the nonocclusive thrombus shown in Fig. 3 progresses to 0.12 mm^3 [Fig. 8(b)].

The same analysis was performed for thrombi grown in the femoral vein. Calculating Gc for an occlusive thrombus and fitting the calculated matrix into the dimension of the femoral vein, resulted in the calculation

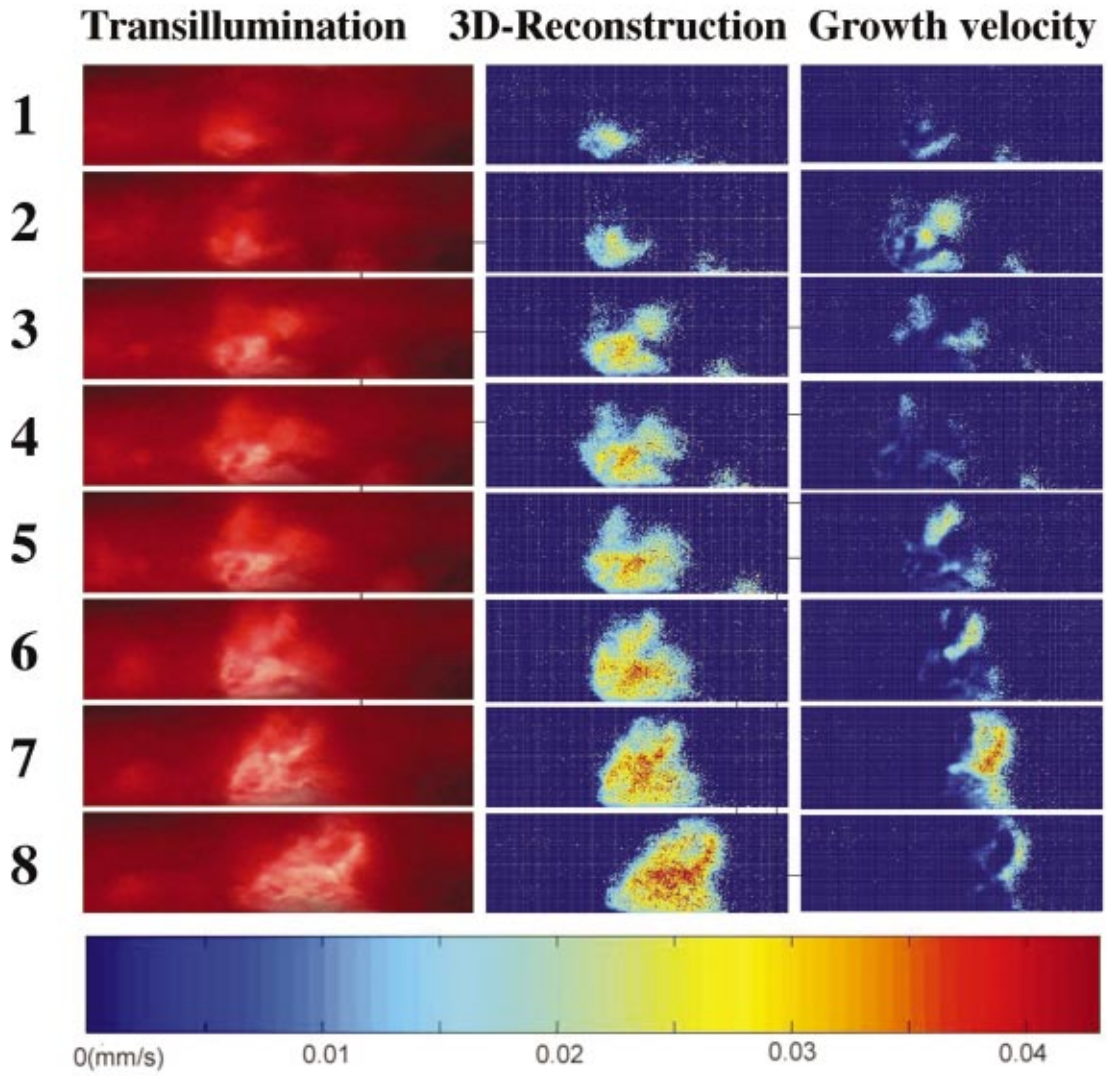

FIGURE 3. 3D-reconstructed images of thrombosis and calculation of growth velocity. Reconstruction of third dimension of thrombus formation (middle column) from a series of sequential images (first column) obtained in the hamster carotid artery, following photochemical injury induction; the calculated growth velocity is shown in the third column and has to be added to the middle picture of the same row to achieve the middle picture of the next row. The thrombus starts to move in the last two pictures due to increasingly strong flow. Reconstructed images are shown in top view and a graded color scale bar for the representation of the thrombus growth velocity is shown at the bottom of the figure.

of a conversion factor of $190 \pm 10\ \mu$m. This factor is identical to that determined for the carotid artery and confirms that Gc has effectively eliminated the transmissivity of the vessel wall, different for arteries and veins. Finally, Fig. 8(c) shows the real volume evolution with time of the femoral vein thrombus shown in Fig. 5.

DISCUSSION

Studying thrombus formation via transillumination of a blood vessel offers the advantage that, in addition to providing kinetic information, thrombus formation can be visualized on-line. The thrombus formed in our model has been quantified via measuring the light intensity of the transilluminated light, which is proportional to the amount of non-colored platelets in the thrombus.[21,22] In the present study, an effort was made to further quantitatively manage this process by applying a matrix analysis on our images, enabling a reconstruction of thrombosis in three dimensions. This analysis was validated by selecting examples of occlusive thrombi, the reconstructed images of which could be fitted to the dimensions of the blood vessels studied. This approach therefore enabled us to calculate true thrombus volumes and to study the kinetics of thrombus growth in relation to the location and three-dimensional geometry of the

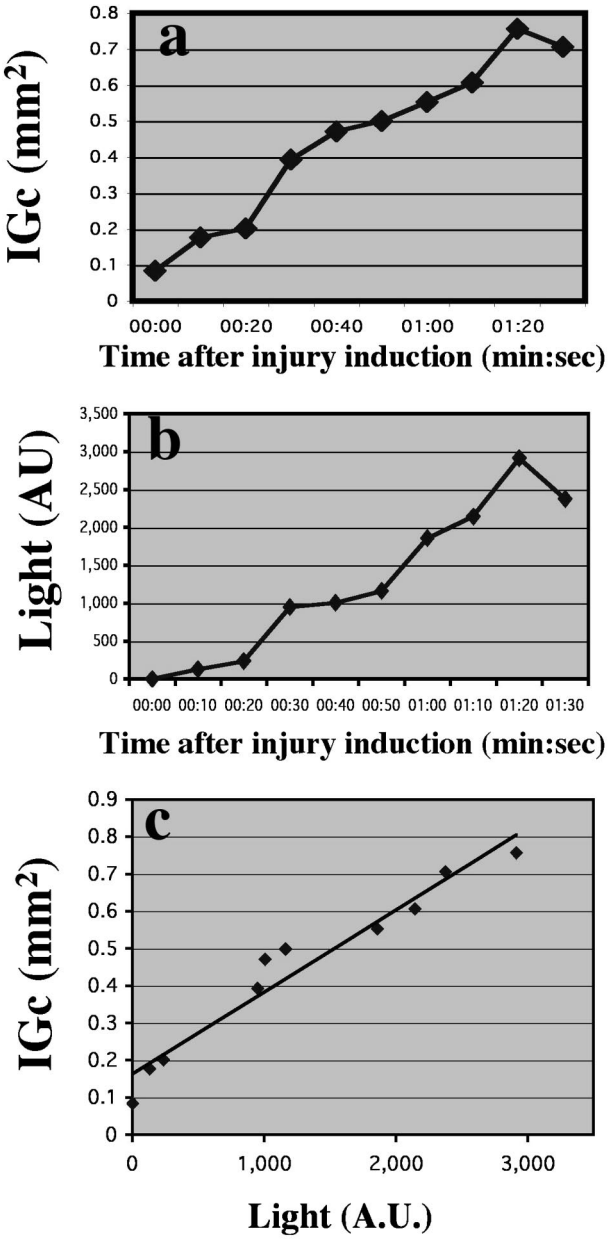

FIGURE 4. Evolution of thrombus growth parameters IGc and light intensity. The calculated IGc for the thrombus shown in Fig. 3 is represented as a function of time (a) in parallel with the calculated arbitrary light intensity, expressed in A.U. (b); linear correlation between IGc and A.U. (c).

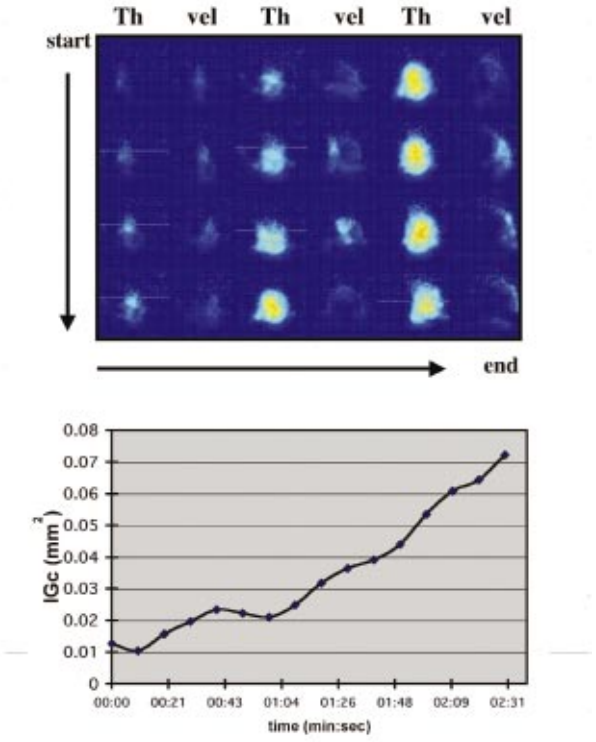

FIGURE 5. Evolution of venous thrombosis in the hamster. Sequential 3D-reconstructed images of thrombus (Th) formation in the femoral vein of the hamster in conjunction with the derived growth velocity (vel) (upper panel); plot of IGc vs time during this venous thrombus development (lower panel).

growing thrombus. We found that the integration of Gc over the full field resulted in a mathematically derived parameter IGc, which is linearly related to real thrombus volumes, but our method suffers from one conceptual limitation. Since a 3D configuration is calculated from a 2D picture, holding information on the third dimension, the reconstruction had to be done arbitrarily, either bottom-up or top-down. Therefore, although our graphical representation of the third dimension may not be entirely correct in all circumstances, our analysis will still provide correct volumetric and kinetic information for the developing thrombi.

The highly proportional correlation between the thrombus size, expressed in arbitrary light units and the matrix-derived parameter IGc, confirmed that the matrix analysis provided the correct numerical information to reconstruct the thrombus. This may not seem surprising because both analyses use the same thrombus images, yet are conducted in an entirely different manner. This correlation therefore allowed the further volumetric transformation of IGc in a true thrombus volume. These transformations relied on estimates of the inner diameter of the blood vessel from histological cross sections (error margin of 5%) and on an estimate of the area per pixel in the setup used (error margin of 10%). Therefore, the error of IGc is around 10%. Further taking into account an error margin of 5% on the *conversion factor* (related to the error on the blood vessel diameter and that on Gc), the overall error of the volume calculation is estimated to be around 15%.

Essentially no difference was found in the volumetric analysis of platelet-rich arterial and venous thrombi, despite the different geometry of the vessel wall. Identical

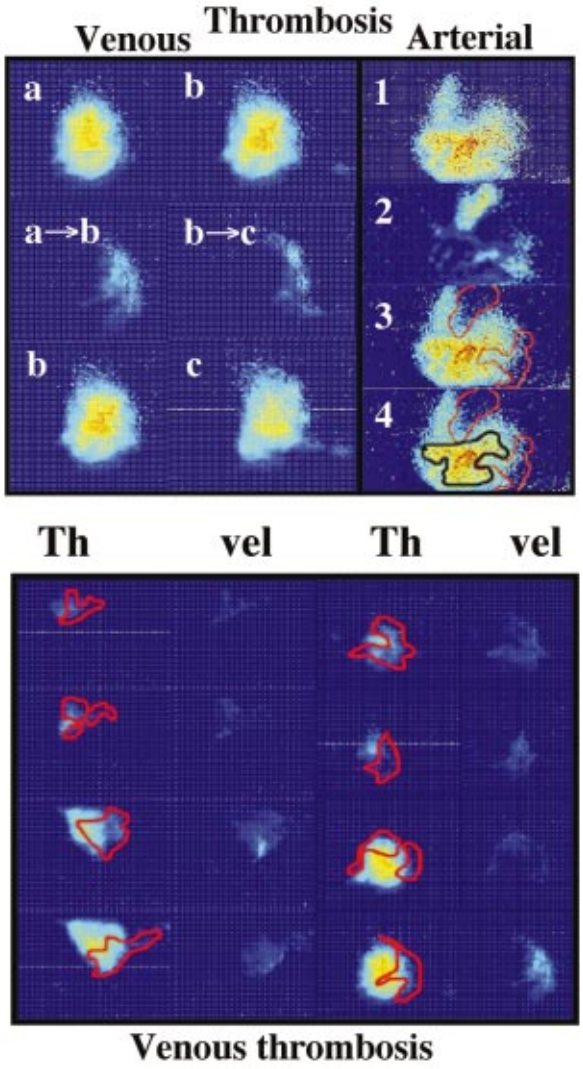

FIGURE 6. Thrombus growth is at the tailing end. Detailed images of arterial and venous thrombus growth (vel) as indicated, in comparison to the 3D-reconstructed thrombus (Th) masses a, b, and c, respectively; the growth velocity is highest in regions of disturbed flow (1–3) and not in the area of the highest shear forces (4); the rapidly growing area (velocity>0.01 mm s^{-1}) is marked in red contours and the areas of relative higher shear forces (thickness>0.2 mm) in black contours.

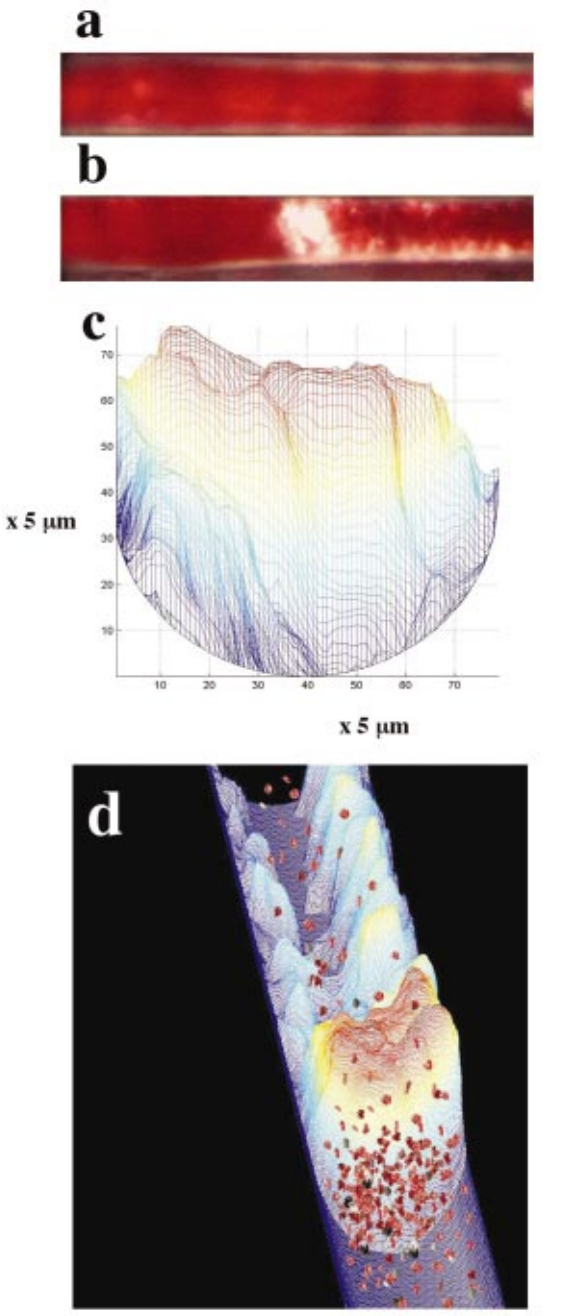

FIGURE 7. Thrombus reconstruction of occlusive arterial thrombosis. Representative pictures of a thrombus occluding the hamster carotid artery (b) and of the vessel wall prior to thrombosis (a); corresponding 3D reconstructions of the thrombus in front view (c), and in sideview (d). Red blood cells have been added to represent blood flow.

conversion factors were found, further confirming that the matrix Gc no longer depends on the transmissivity of the blood vessel. The further comparison of the calculated real volumes and the corresponding arbitrary light units for the corresponding thrombus, then reveal that 1000 A.U. approximately represent a thrombus volume of 0.03 mm^3. It should be stressed that in the present study thrombi were fitted to standardized blood vessel diameters, as determined on histochemical cross sections. Since thrombus development can be associated with arterial contraction, or veins can dilate during their manipulation, the true inner diameter of the transilluminated vessels that were selected for the fitting in the present study, may slightly diverge from the standardized histological diameter chosen. A completely correct fitting, therefore, would require an exact estimate of the inner diameter of those vessels used in the fitting; a correct conversion factor applicable in all carotid artery experi-

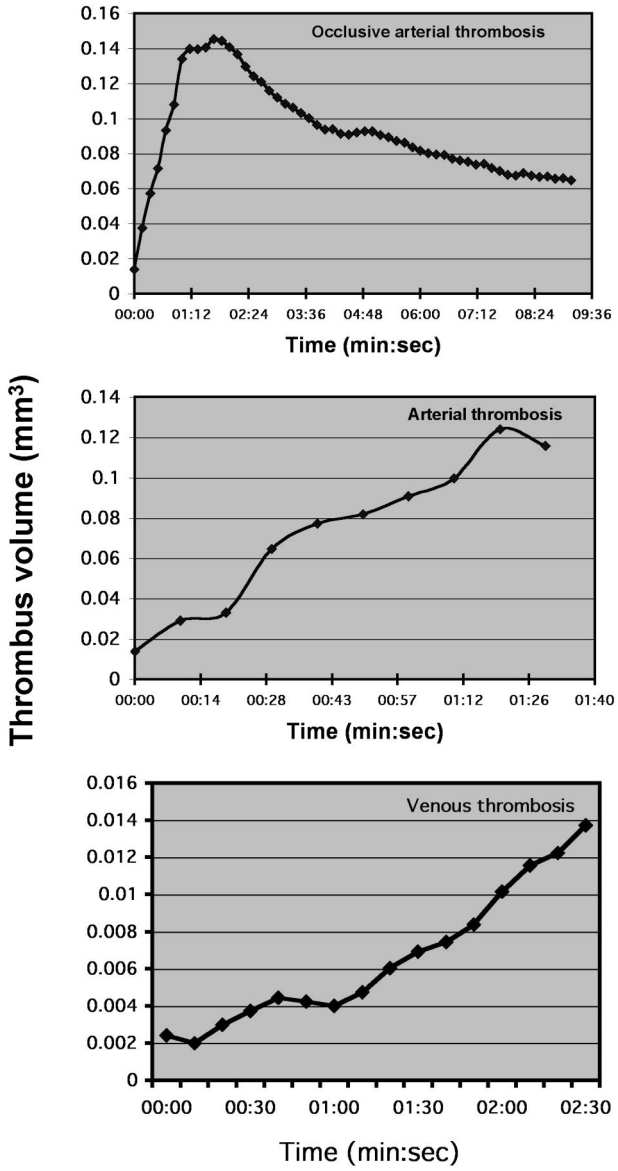

FIGURE 8. Real volume development during thrombosis. Progression of arterial and venous thrombosis as indicated, after conversion of IGc into real thrombus volumes.

ments could then be calculated as follows: 190 μm $\times$ true diameter/0.45 mm. To further experimentally approach this question, we had removed hamster carotid artery thrombi, which following fixation were further studied via confocal microscopy. However, removal of the thrombosed blood vessel resulted in its shrinking and a complete 3D reconstruction of the thrombus interior parts of the thrombus appeared to be impossible, in view of the large thrombus diameters. Hence, the present analysis of occlusive thrombi appeared to be the only feasible approach in the definition of the geometrical factors required for our volumetric analysis.

In addition to providing a 3D reconstruction for thrombus volume estimation, our present analysis also provided us with a tool to visualize the kinetics of thrombus growth *in vivo*, enabling the study of secondary processes involved in platelet aggregation during thrombus growth. Such analysis has shown that the growth of small thrombi occurs in a random fashion. Venous thrombi especially grow randomly, in agreement with a fairly low flow rate in the venous circulation, although at higher thrombus volumes, thrombus growth preferentially occurs in the tailing vortex of the thrombus. In the arterial circulation, on the contrary, thrombus growth preferentially occurs at one end of the thrombus in a zone of recirculating flow and does not seem to occur in those areas where the shear forces are most elevated, as can be visualized in 3D-reconstructed thrombi. Thus, these findings confirm *in vitro*[2,16] and *in vivo*[9,13,15] data on thrombus development in disturbed flow, reporting that the fast-growing area is usually located in the tailing vortex of blood flow, due to the concentration of platelets in this area and eddy flow responsible for platelet impact and interaction.

In conclusion, the present mathematical analysis of an existing animal model of thrombosis has enabled us to reconstruct thrombosis in three dimensions and to study the kinetics of thrombus growth in more detail in an *in vivo* setting. This image treatment may, therefore, be useful for the analysis of biorheological aspects of thrombosis in vivo, and provide a tool to study specific antiplatelet drugs with different modes of action, distinguishing between inhibition of platelet aggregation and adhesion.

ACKNOWLEDGMENTS

The authors are grateful to Ingrid Vreys for skillful technical assistance during the preparation of the *in vivo* experiments analyzed in the present study. The financial support of the Flemish Fund for Scientific Research FWO Vlaanderen Project G 0376.01 is highly acknowledged.

NOMENCLATURE

Gc	nondimensional gray-compensated parameter
IGc	integrated Gc (sum of Gc, multiplied by area per pixel, resulting in a dimension of mm^2)
P	transmitted light intensity through the blood vessel at a certain point
P_c	transmitted light intensity at a corresponding point on the compensation picture
μ	transmissivity
D	diameter of the blood vessel
d	thickness

REFERENCES

[1] Angelillo-Scherrer, A., P. de Frutos, C. Aparicio, E. Melis, P. Savi, F. Lupu, J. Arnout, M. Dewerchin, M. F. Hoylaerts, J. Herbert, D. Collen, B. Dahlback, and P. Carmeliet. Deficiency or inhibition of Gas6 causes platelet dysfunction and protects mice against thrombosis. *Nat. Med.* 7:215–221, 2001.

[2] Barstad, R. M., H. E. Roald, Y. Cui, V. T. Turitto, and K. S. Sakariassen. A perfusion chamber developed to investigate thrombus formation and shear profiles in flowing native human blood at the apex of well-defined stenoses. *Arterioscler. Thromb.* 14:1984–1991, 1994.

[3] Bernat, A., P. Hoffmann, and J. M. Herbert. Antagonism of SR 90107A/Org 31540-induced bleeding by protamine sulfate in rats and mice. *Thromb. Haemostasis* 76:715–719, 1996.

[4] Cho, J. H., C. H. Yun, H. S. Seo, T. Koga, T. Dan, B. A. Koo, and H. Y. Kim. The antithrombotic efficacy of AT-1459, a novel, direct thrombin inhibitor, in rat models of venous and arterial thrombosis. *Thromb. Haemostasis* 86:1512–1520, 2001.

[5] Davies, M. S., and A. C. Thomas. Plaque fissuring: the cause of acute myocardial infarction, sudden ischaemic death, and crescendo angina. *Br. Heart J.* 53:363–373, 1985.

[6] Fay, W. P., J. G. Murphy, and W. G. Owen. High concentrations of active plasminogen activator inhibitor-1 in porcine coronary artery thrombi. *Arterioscler., Thromb., Vasc. Biol.* 16:1277–1284, 1996.

[7] Giles, A. R. Guidelines for the use of animals in biomedical research. *Thromb. Haemostasis* 58:1078–1084, 1987.

[8] Hartwell, D. W., and D. D. Wagner. New discoveries with mice mutant in endothelial and platelet selectins. *Thromb. Haemostasis* 82:850–857, 1999.

[9] Karino, T., and H. L. Goldsmith. Role of blood cell-wall interactions in thrombogenesis and atherogenesis: A microrheological study. *Biorheology* 21:587–601, 1984.

[10] Kawasaki, T., M. Dewerchin, H. R. Lijnen, J. Vermylen, and M. F. Hoylaerts. Vascular release of plasmiogen activator inhibitor-1 imparis fibrinolysis during acute arterial thrombosis in mice. *Blood* 96:153–160, 2000.

[11] Kawasaki, T., T. Kaida, J. Arnout, J. Vermylen, and M. F. Hoylaerts. A new animal model of thrombophilia confirms that high plasma factor VIII levels are thrombogenic. *Thromb. Haemostasis* 81:306–311, 1999.

[12] Keller, J. W., and J. D. Folts. Combined inhibitory effects of aspirin and ethanol on adrenaline exacerbation of acute platelet thrombus formation in stenosed canine coronary arteries. *Cardiovasc. Res.* 24:191–197, 1990.

[13] Lassila, R., J. J. Badimon, S. Vallabhajosula, and L. Badimon. Dynamic monitoring of platelet deposition on severely damaged vessel wall in flowing blood. Effects of different stenoses on thrombus growth. *Arteriosclerosis (Dallas)* 10:306–315, 1990.

[14] Libby, P. Current concepts of the pathogenesis of the acute coronary syndromes. *Circulation* 104:365–372, 2001.

[15] Liu, S. Q., L. Zhong, and J. Goldman. Control of the shape of a thrombus-neointima-like structure by blood shear stress. *J. Biomech. Eng.* 124:30–36, 2002.

[16] Marchese, P., E. Saldívar, J. Ware, and Z. M. Ruggeri. Adhesive properties of the isolated amino-terminal domain of platelet glycoprotein Iba in a flow field. *Proc. Natl. Acad. Sci. U.S.A.* 96:7837–7842, 1999.

[17] Matsuno, H., T. Uematsu, S. Nagashima, and M. Nakashima. Photochemically induced thrombosis model in rat femoral artery and evaluation of effects of heparin and tissue-type plasminogen activator with use of this model. *J. Pharmacol. Methods* 25:303–317, 1991.

[18] Nemmar, A., M. F. Hoylaerts, E. Verbeken, P. H. M. Hoet, and B. Nemery. Utrafine particles affect experimental thrombosis *in vivo*. *Am. J. Respir. Crit. Care Med.* 166:998–1004, 2002.

[19] Ni, H., C. V. Denis, S. Subbarao, J. L. Degen, T. N. Sato, R. O. Hynes, and D. D. Wagner. Persistence of platelet thrombus formation in arterioles of mice lacking both von Willebrand factor and fibrinogen. *J. Clin. Invest.* 106:385–392, 2000.

[20] Sprawls P. In: Physical Principles of Medical Imaging, Madison, WI: Medical Physics, 1995.

[21] Stockmans, F., J. M. Stassen, J. Vermylen, M. F. Hoylaerts, and Å. Nyström. A technique to investigate mural thrombus formation in small arteries and veins: I. Comparative morphometric and histological analysis. *Ann. Plast. Surg.* 38:56–62, 1997.

[22] Stockmans, F., J. M. Stassen, J. Vermylen, M. F. Hoylaerts, and Å. Nyström. A technique to investigate mural thrombus formation in small arteries and veins: II. Effects of aspirin, heparin, r-hirudin and G-4120. *Ann. Plast. Surg.* 38:63–68, 1997.

[23] Takiguchi, Y., K. Wada, H. Matsuno, and M. Nakashima. Effect of diabetes on photochemically induced thrombosis in femoral artery and platelet aggregation in rats. *Thromb. Res.* 63:445–456, 1991.

[24] Umemura, K., Y. Kohno, H. Matsuno, T. Uematsu, and M. Nakashima. A new model for photochemically induced thrombosis in the inner ear microcirculation and the use of hearing loss as a measure for microcirculatory disorders. *Eur. Arch. Otorhinolaryngol.* 248:105–108, 1990.

[25] Wu, D., M. Meiring, H. F. Kotze, H. Deckmyn, and N. Cauwenberghs. Inhibition of platelet glycoprotein Ib, glycoprotein IIb/IIIa, or both by monoclonal antibodies prevents arterial thrombosis in baboons. *Arterioscler., Thromb., Vasc. Biol.* 22:323–328, 2002.

[26] Yamamoto, H., I. Vreys, J. M. Stassen, R. Yoshimoto, J. Vermylen, and M. F. Hoylaerts. Antagonism of vWF inhibits both injury induced arterial and venous thrombosis in the hamster. *Thromb. Haemostasis* 79:202–210, 1998.